A New Method for MPPT Algorithm Implementation and Testing, Suitable for Photovoltaic Cells

Alexandru SFIRAT, Aurel GONTEAN, Szilard BULARKA
Polithenica University of Timisoara, Applied Electronics Department, Timişoara, 300006, Romania
alexandru.sfirat@student.upt.ro, aurel.gontean@upt.ro, szilard.bularka@student.upt.ro

***Abstract*—The goal of this paper is to present an implementation method for a Maximum Power Point Tracking (MPPT) algorithm using an electronic load and custom designed LabView software. The aim is to facilitate the testing of the algorithm in laboratory conditions, before it can be used in the real world, improving development time, facilitating cost reduction and offering confidence in the design. This paper analyses the most suitable MPPT algorithms for testing purposes and suggests a complete software and hardware implementation for hardware in the loop testing which can facilitate in-depth evaluation of different algorithms. In order to replicate realistic stimuli for the MPPT algorithm, a solar array simulator has been designed. Using the proposed method, the performance of various MPPT algorithms for different atmospheric conditions can be evaluated. The hardware and software setup have been tested and validated in laboratory conditions. The experimental results have validated the proposed evaluation method and the good dynamic response of the MPPT algorithm.**

***Index Terms*—algorithms, maximum power point trackers, photovoltaic cells, simulation, solar energy.**

I. Introduction

The depletion of fossil fuels and the problems associated with them, along with the climate changes led to an increased demand for renewable energies sources in the last decades. Among these sources, photovoltaics (PV) own an important share. The complete design of such a complete PV system involves major challenges in the design and analysis of the efficiency of the system [1]. PV energy has been attracting more attention in the last years, as it met the requirement of being environmentally compatible and resource conserving.

Due to changing atmospheric conditions, temperature and self-heating, the output of the PV cells are continuously changing and a smart algorithm that monitors and adapts the input load to the output parameters of the PV cells is mandatory to improve the overall efficiency of the whole system. MPPT algorithms are therefore the key points in designing and improving the efficiency of such a system.

PV cells allow the energy transported by the electromagnetic waves (i.e., photons) to be directly converted into electricity [2]. The mechanism that allows this type of energy conversion to take place is based on photoelectron interactions that occur in P-N junctions formed by appropriately doped semiconductor materials. Hybrid systems that use solar power together with heat absorption techniques using thermoelectric generators are also commonly used [2].

PV modules have a nonlinear current-voltage characteristic with a unique point where the produced power is maximum [3], which leads to the need for an algorithm that identifies and keeps the system at this point.

MPPT algorithms are necessary, first of all, to place the power transfer between the PV module and the load in the best case scenario, thus increasing the efficiency of the system.

An innovative method for implementing and testing a MPPT algorithm in laboratory conditions within a moderate budget is presented in the next sections.

II. Photovoltaic Cell Model Review and MPPT Algorithms Analysis

A. Photovoltaic Cell Model

The classical single diode electrical model for the silicon PV cell is presented in Fig. 1. As opposed to the real cell, the ideal model does not take into consideration the internal parasitic resistances R_s and R_{sh}.

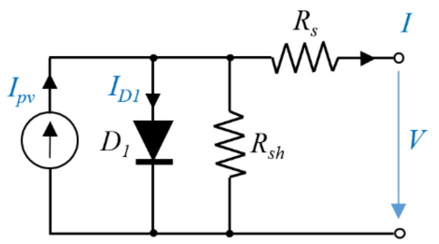

Figure 1. Equivalent electrical circuit for the PV cell (module)

Equation (1) gives the I-V relation between the output current I and the output voltage V for the single diode model:

$$I = I_{pv} - I_0 \left[\exp\left(\frac{qV}{nN_s k_B T} \right) - 1 \right] \tag{1}$$

where I_{PV} is the photonic generated current, I_0 is the reverse saturation diode current, q is the absolute value of electron charge, n is the diode ideality factor, N_S represents the number of series PV cells in a module, k_B is the Boltzmann constant and T is the internal temperature of the cell.

Writing the Kirchhoff Current Law in the schematic from Fig. 1, Gray [4] derives the more accurate expression (2):

Digital Object Identifier 10.4316/AECE.2018.03008

$$I = I_{pv} - I_0\left[\exp\left(\frac{q(V+IR_s)}{nN_s k_B T}\right)-1\right]-\frac{V+IR_s}{R_{sh}} \tag{2}$$

Saloux *et al.* [2] show by comparing the equations of the ideal and real PV cell models that the series resistance R_s affects the output voltage, while the shunt resistance R_{sh} reduces the available electrical current.

Dey *et al.* [5] express the photovoltaic current, I_{PV}, like in equation (3):

$$I_{pv} = \left[\mu_{SC}\left(T_c - T_{ref}\right)+I_{sc}\right]\frac{G}{G_{ref}} \tag{3}$$

where μ_{SC} is the short circuit current temperature coefficient, T is the internal temperature of the PV cell, T_{ref} is the reference temperature (298.15K), G is the current irradiance and G_{ref} is the reference irradiance (1000 W/m^2).

B. *Maximum Power Point Tracking Algorithms*

The typical I-V and P-V characteristic curves presented in Fig. 3 are the basis of multiple MPPT algorithms analysis developments and integration (in Fig. 3 we considered $N_S = 10$).

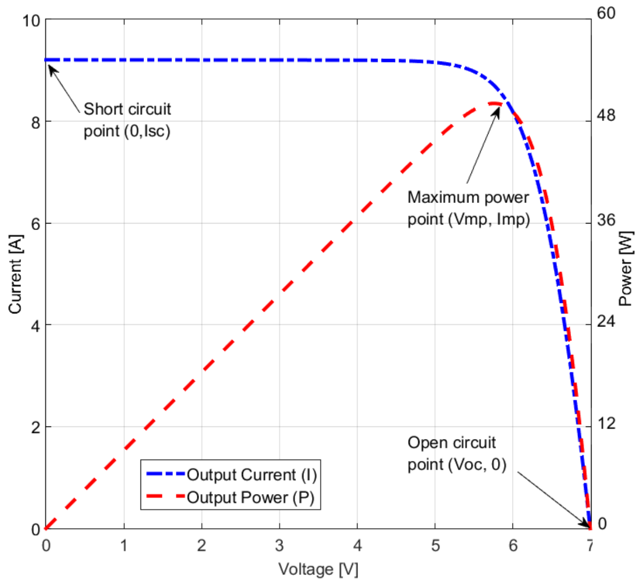

Figure 3. Typical I-V and P-V characteristic curves of a PV cell module

As stated also in [5-6] and presented in Fig. 3, the most important points of interest of any PV cell or module for the MPPT algorithms are: the short circuit current $I_{sc;}$ the open circuit voltage $V_{oc;}$ MPP, with the corresponding current I_{mp} and voltage, V_{mp}. The power at this point is the maximum that the PV module is able to deliver.

The purpose of these algorithms is to detect a change in the output parameters of the PV device and to adapt the input parameters of the load to these new conditions in such a way that the power transfer between the PV device and the load will continuously be at the maximum level. As stated in [3], the location of the MPP point is not known a priori. This point has to be calculated either by using the model parameters or by using a search algorithm. The situation is further complicated by the fact that the MPP depends in a nonlinear way on irradiance, as shown in Fig. 4.

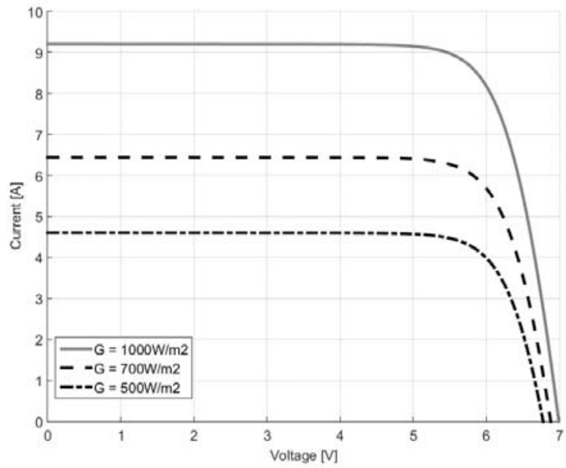

Figure 4. I-V characteristic curves of a PV module at different irradiances

Based on these requirements, several algorithms have evolved and were implemented and tested [7]. The most common MPPT algorithms are: Perturb and observe (P&O); Incremental conductance (IC); Current sweep (CS); Constant voltage (CV); The P&O algorithm [7,10] is one of the simplest and also commonly implemented and used. The main idea of this algorithm is to increase the PV device voltage with a predefined step and to measure the power after each increase. The Incremental Conductance (IC) algorithm [8] is more sophisticated compared to the P&O algorithm and is also more efficient. The main idea of the incremental conductance algorithm is to monitor the change in power and consider that at the MPP point, dP/dV equals to zero. The Current Sweep algorithm uses a sweep waveform of the output voltage of the PV module at fixed intervals of time. Based on the obtained waveform, the MPP point is calculated and extracted [9].The Constant Voltage algorithm [3], is based on the fact that the ratio of the array's maximum power voltage, V_{mp}, to its open-circuit voltage V_{oc}, is approximately constant.

In this paper, the authors are focusing on analyzing, implementing and testing the Incremental Conductance algorithm, as is it is one of the algorithms that adapt very fast to the changing atmospheric conditions and has a good efficiency [10-13].

III. INCREMENTAL CONDUCTANCE MPPT ALGORITHM

The logic diagram of such an algorithm is presented in Fig. 5 (the initial phase) and in Fig. 6 (the whole process).

The main idea of an incremental conductance MPPT algorithm is based on the following equation:

$$\left.\frac{\mathrm{d}P}{\mathrm{d}V}=0\right|_{\text{at MPP}} \tag{4}$$

Equation (4) points that at the MPP, the derivative of the power with respect to voltage equals to zero. Equation (4) can be written as follows (5):

$$\left.\frac{\mathrm{d}(VI)}{\mathrm{d}V}\right|_{\text{at MPP}} = I + V\frac{\mathrm{d}I}{\mathrm{d}V}=0 \tag{5}$$

Rewriting (5) as (6) gives:

$$\frac{dI}{dV} = -\frac{I}{V} \tag{6}$$

Based on relations (6, 6a, 6b), the algorithm can detect if there was a change in the atmospheric conditions, which translates in a change in voltage or in current. Relations (6a) and (6b) provide the direction in which the IC algorithm should move (increased/decreased voltage) in order to maintain the MPP.

$$\frac{dP}{dV} > 0 \text{ (increased voltage)} \quad (6a)$$

$$\frac{dP}{dV} < 0 \text{ (decreased voltage)} \quad (6b)$$

The algorithm will monitor the output voltage and output current of the PV device and based on the current and previous voltage values will detect a change in the output parameters. In order to maintain the output at MPP, the module's operating voltage will be adjusted based on a previously defined step. The operating voltage of the module can be adjusted by updating the constant voltage (CV) setting of an Eload for example.

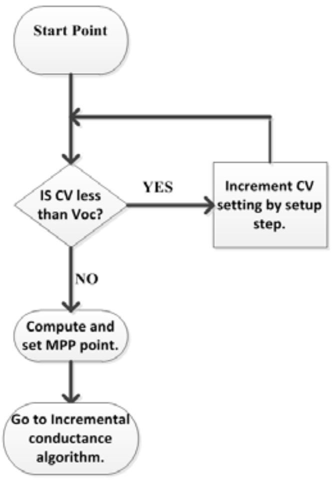

Figure 5. Initial phase of Incremental Conductance algorithm block diagram

In case that $dV = 0$ and $dI = 0$, there is no change in the voltage nor the current and the algorithm is still operating at the MPP. If $dV = 0$ and $dI > 0$, it means that the current of the PV device has increased and the operating voltage must be also increased to maintain the MPP. Vice versa, if $dI < 0$, the output current has decreased and the operating voltage must also be decreased with the same goal of maintaining the MPP.

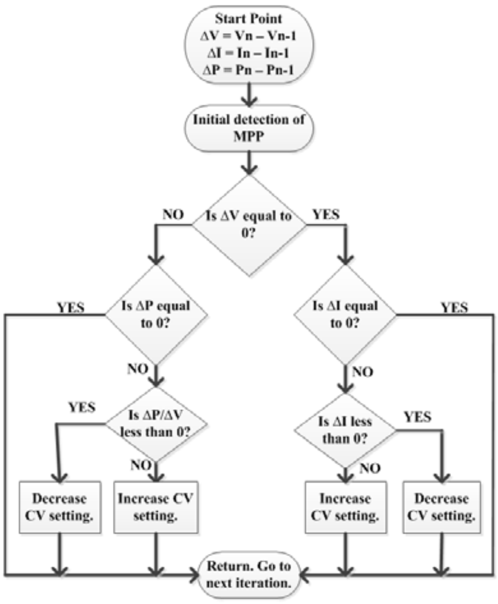

Figure 6. Incremental Conductance algorithm block diagram

In case that there was a variation in the output voltage $dV \neq 0$, relying on relations (6a) and (6b), the algorithm will act as follows: if $dP/dV < 0$, the operating voltage is to the right of the MPP and the operating voltage must be decreased. Vice versa, if $dP/dV > 0$, the operating voltage is to the left of the MPP and the operating voltage must be increased. Fig. 5 describes the initial phase of the incremental conductance algorithm. In order to detect the current MPP, a sweep from 0 to V_{oc} has to be run. The output voltage and current must be saved and computed in such a way that the initial MPP point is detected.

IV. Solar Array Simulator Design

A solar array simulator (SAS) is a device which emulates I-V curves in order to test the MPPT algorithm. Various SAS implementations can be found in literature [14-17].

In our case a PV module containing multiple series cells with the parameters presented in Table I were simulated using LTSpice and emulated using a custom built SAS [18-20].

TABLE I. EXPERIMENTAL PHOTOVOLTAIC CELL PARAMETERS [31]

Parameter	Symbol	Value
Maximum Power	P_{mp}	5.01 W
Open-circuit voltage	V_{OC}	0.699 V
Operating Voltage	V_{mp}	0.572 V
Short-circuit Current	I_{SC}	9.206 A
Operating Current	I_{mp}	8.756 A
Conversion Efficiency		Up to 21%
Size		156 x 156 mm
Material		Monocrystalline Silicon

The simplest method for obtaining the I-V characteristic of a PV cell or array is to use, as a starting point, the reverse characteristic of a silicon diode. The basic simulation circuit is presented in Fig. 7, where several diode types were tested until a proper fit was found [21-23].

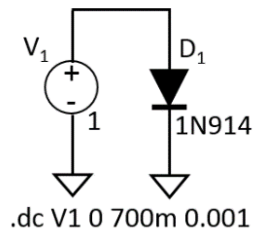

Figure 7. Simulation schematic for the silicon diode transfer characteristic

If a single PV cell is considered, the modeled I-V characteristic of the cell can be expressed by equation (7):

$$I_{pv} = I_{sc} - \psi I_D(V) \quad (7)$$

where I_{pv} is the photovoltaic current, I_{sc} is the short circuit current of the PV cell, I_D is the current through the diode and ψ is an empirical constant, computed to 820 in our case. In (7) I_{sc} is a parameter from which a multiple of I_D is subtracted – this procedure explains the term "reversed diode" we use. The I-V characteristic of the simulated circuit is presented in Fig. 8, where the data was extracted from the corresponding LT Spice simulation.

The I-V and the P-V characteristics of the reverse diode are very similar to the characteristics of the PV cell presented in Figure 3. To further compare the results, figure 9a plots the I-V characteristics of the reversed diode model vs the actual PV cell data, while figure 9b represents the corresponding P-V characteristics.

The PV cell parameters were thoroughly studied in previous work [24] and an accurate model was obtained. Based on these previous results, we analyzed, designed and implemented a SAS using the above findings.

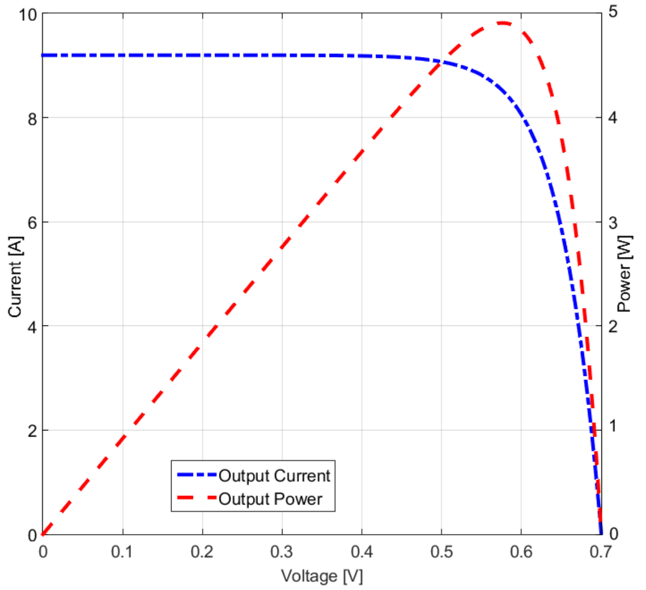

Figure 8. The PV cell modeled I-V and P-V characteristics

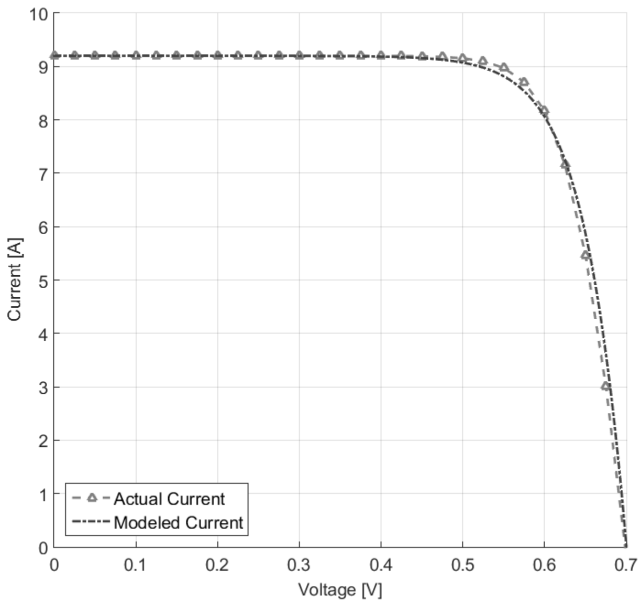

Figure 9a. Reversed diode modeled current vs actual current for a PV cell

The block diagram of the SAS is presented in Fig. 10. The load voltage V is conditioned according to the modeled PV cell characteristic using a feedback voltage V_{FB} determined by the load current. Based on the V_{FB} voltage, the V-I convertor generates the corresponding I current.

In Fig. 11, the basic schematic of a SAS that uses the characteristic of the reverse silicon diode D_1 is presented.

The load is R_5 and its value was modified in simulations in order to derive the electrical characteristics of the SAS. U4 and Q1 control the current through D1 relative to the load current. U2 operates as a differential amplifier having the output voltage proportional to the D1 current.

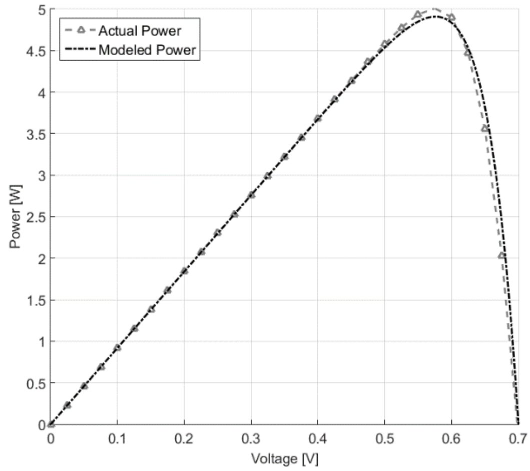

Figure 9b. Reversed diode modeled power vs actual power for a PV cell

The ratio between R14 and R13 provides the I_{sc} current value. G1 is the voltage to current convertor (controlled by the U1 summing inverter) and is used to generate the output load current.

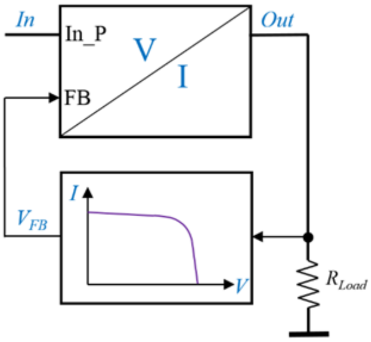

Figure 10. Block diagram of a basic SAS

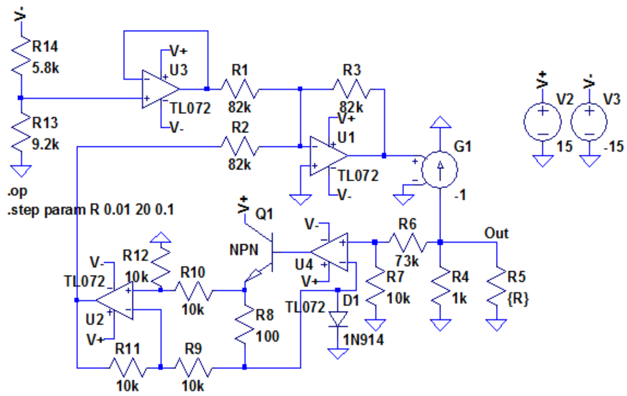

Figure 11. SAS based on the characteristics of a silicon diode – basic schematic

The circuit has been simulated in LT Spice and the generated I-V and P-V characteristics are presented in Fig. 12. The values of the output current and output voltage corresponding to ten PV cells connected in series, therefore the short circuit current is set at 9.206A and the output open circuit voltage is around 7 V.

The main purpose of the SAS is to generate a family of I-V curves that will be fed at the input of the MPPT algorithm implemented in the load simulator. In this way, the atmospheric conditions that affect the output of the PV cells are simulated in laboratory conditions, and this can be easily achieved by changing the ratio between R14 and R13.

The authors have prototyped a simple and inexpensive SAS having the block diagram represented in Fig. 13. The practical implementation of the solar simulator was based on the idea from J. Clarke [25].

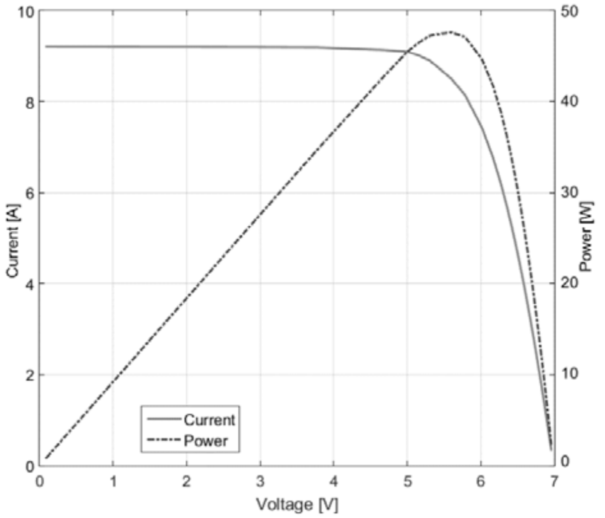

Figure 12. Solar array simulator based on the I-V characteristics of a silicon diode – output characteristics

IC3 is a linear error amplifier which drives Q1, a power pMOS. Multiple MOSFETs can be used in order to increase the output current of the SAS. IC1 monitors the current through the output using the shunt resistance RS. In order to properly simulate a PV module, a special topology was used (IC1 and IC2 controlling IC3). IC2 is used for setting the output current limit (I_{sc}) and it also controls the rate at which the output voltage drops off when it is reached. IC4 provides a variable reference for IC3 (V_{oc}).

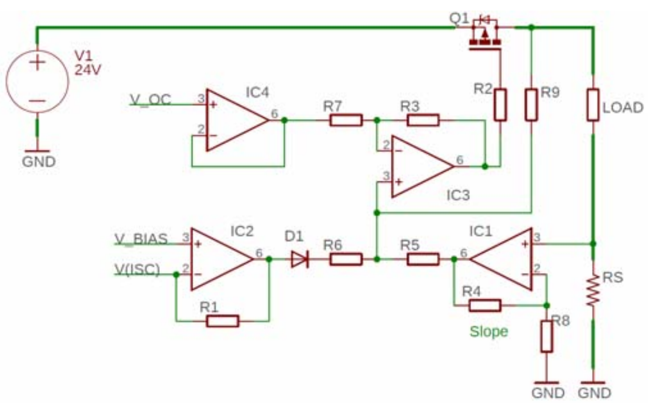

Figure 13. Solar array simulator schematic block diagram

In order to generate the real characteristics of our SAS, a dedicated setup was used, consisting of an electronic load and the corresponding software. The electronic load offers the advantage of being easily controlled by software. The application sweeps the constant voltage setting (CV) from zero to V_{oc} in order to continuously measure the output voltage and the output current. Based on these measurements the output power is computed. The measured P-V and I-V characteristics of the SAS are presented in Fig. 14. The plot is generated by our LabVIEW application and proves to be similar to the simulated one (in the particular case of our implemented SAS, $N_S = 7$).

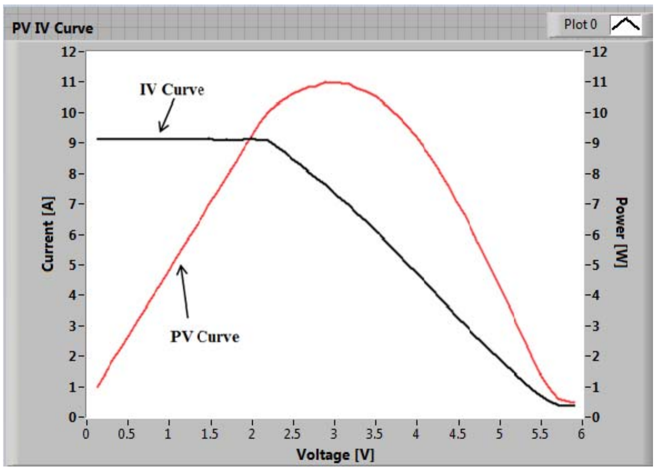

Figure 14. Implemented SAS P-V and I-V output characteristic

In this scenario, the SAS was set to generate a maximum current of 9.206A and the open circuit voltage was set to 4.9V. The output characteristic of the SAS can be modified by varying the value of two potentiometers: the first is connected to the *V_oc* input of IC4 and the second to the *V(ISC)* inverting input of IC2.

The dissipated power over Q1 can become very large. For example, when the SAS operates close to the short-circuit point, the dissipated power reaches up to 240W, even in the situation when a medium-sized PV panel is simulated. This approach is both inefficient and difficult to be used, so fixes had to be investigated.

One possible solution, also implemented in power supply designs, is to use a tracking pre-regulator in the voltage loop (Fig. 15). The pre-regulator is continuously adjusting its output voltage so it remains at the $V_{Load} + V_1$ level, where V_1 is the intended Q1 drop-off voltage (typically around 2 to 4V). In this case, the dissipated power over Q1 drops to a moderate level of 20 … 40W.

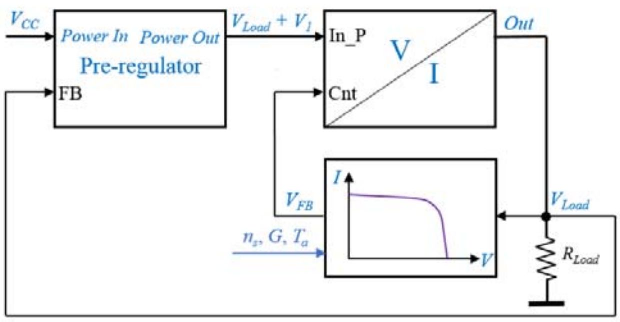

Figure 15. I-V Solar array simulator with the tracking pre-regulator

V. Implementation Of The MPPT Algorithm Using An eLoad And A LabVIEW Application

Our MPPT incremental conductance algorithm runs on a standard PC using LabView software. Similar implementations can be found in [26-27].

The algorithm monitors the output current and output voltage of the PV device. It adjusts, if necessary, the operating voltage using the electronic load (operating in constant voltage mode). Predefined values for timings between each measurement and the magnitude of the operating voltage step can be programed by the user.

Choosing a larger value for the operating voltage step will contribute to a faster MPP identification; choosing a smaller value for the operating voltage step will lead to a more accurate MPP finding.

An example of how the algorithm is running using a curve generated by the solar array simulator is presented in Fig. 16.

Assuming that the point on the Curve 1 has been detected by the initial phase of the IC algorithm and that the system is at the MPP (labeled MPP1), if there is a change in the atmospheric conditions the output current is decreasing to Curve 3. The application will detect the change, and based on the incremental conductance algorithm, as described in section III, the voltage setting of the electronic load will be decreased with the predefined step.

The previous action ends with a change in voltage, the next step is to further decrease the voltage setting until dP = 0, which means that the system is at MPP for the new atmospheric conditions (MPP3 on Curve 3).

If another change in the atmospheric conditions will take place, the current will increase from Curve 3 to Curve 2. The system is no longer at the MPP and has to re-adjust the constant voltage setting. As the current has changed and the voltage remains at the same level, the algorithm based on the dI > 0 decision will increase the constant voltage setting. As described above, in previous iteration the voltage has changed, dP has also changed, it means that the dV > 0 and the constant voltage setting will be increased until the system will be again at the MPP (labelled MPP2).

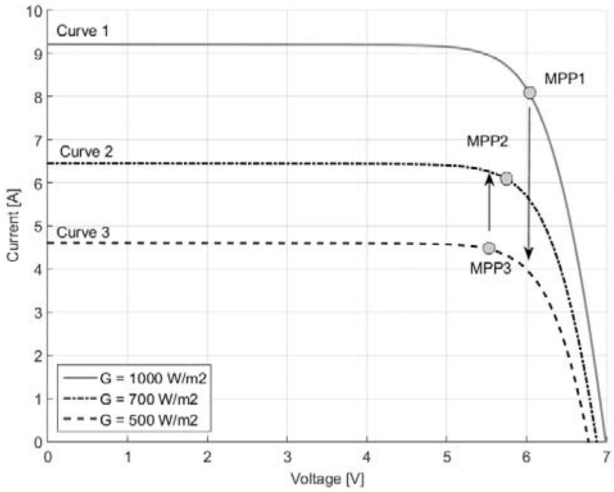

Figure 16. MPPT algorithm example for different irradiance levels

VI. Testing of the MPPT Algorithm using the Solar Array Simulators

A. *Setup for testing maximum point tracking algorithm*

In order to test the performances of the MPPT algorithm under different environmental conditions, a hardware in the loop (HIL) test scheme was implemented. Due to the increasing complexity and short time for development, HIL simulators and test stands gained popularity also in PV system design [28-29]. The main benefit of the proposed method is based on the use of a solar array simulator along with a custom software application, instead of radiation generators and PV cells. The proposed method offers better repeatability and robustness at lower costs, especially at higher power rates, where the generation of uniform radiation is very difficult.

In Fig. 17 the block diagram of the testing system is presented. The solar array simulator as presented in Fig. 13 is controlled by the user to achieve different I-V curves and to simulate real atmospheric conditions.

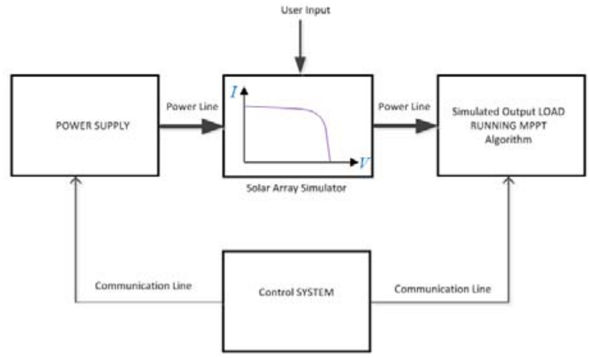

Figure 17. Block diagram of the MPPT algorithm testing system

In Fig. 18 the practical implementation of the testing system for incremental conductance algorithm is presented. The key parts of the system are described below. The electronic load is used for adapting the internal resistance based on the output of the algorithm running on the PC. The electronic load is used in constant voltage mode and the constant voltage setting is used to adapt the MPP algorithm. The solar array simulator is used together with the power supply for simulating the I-V curves. The output parameters of the power supply are controlled from the PC using also a Labview application.

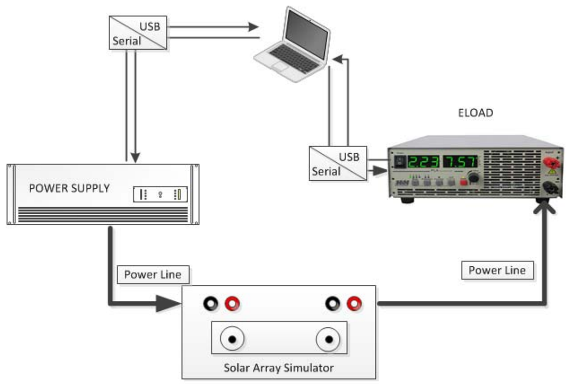

Figure 18. Practical setup of the MPPT algorithm testing system

The electronic load and the power supply are connected to the PC using the serial interface, where the fastest possible baud rate was used (115200).

The electronic load is designed by H&H and has the parameters presented in Table II. In order to simulate a higher power PV module, the HH PLA412 model which has continuous power of 400 W can be selected and used in the desired experiments.

Table II. Electronic Load Parameters [32]

Parameter	Value
Model	HH PLA212
Maximum Voltage	120V
Maximum Current	15 A
Voltage range setting	0 … 120 V
Continuous power	200 W
Short-time power	300 W

B. *Maximum Power Point Tracking Algorithm Application*

The MPPT algorithm has been implemented as a software application designed in LabView. The application has a front panel that is used to adjust various parameters of the algorithm as described below.

The user can set the voltage step, the open circuit voltage and the measurement delay between each iteration. The measurement delay has a major influence on how fast the MPP point is detected. Increasing the value of this parameter, the measurements are more accurate, but the delay until the MPP is reached is higher.

In our particular case, COM8 was selected for communication, using a standard configuration standard 8:N:1.

We collected the necessary data for the amount of steps needed for the IC algorithm to reach the MPP point and the time needed from the moment a new I-V curve was generated and the new MPP point was reached by the application via experiments. The results are listed in Table III. A section for timings and performance measurements will be added in the next software version.

TABLE III. EXPERIMENTAL DATA SHOWING ALGORITHM PERFORMANCE

Exper. #	Voltage setting step value [V]	Measurement delay [ms]	# of steps until MPP	Delay until MPP [ms]
1	0.01	50	not reached	not reached
2	0.1	50	27	1450
3	0.2	50	17	900
4	0.5	50	not reached	not reached
5	0.01	100	200	25000
6	0.1	100	26	3000
7	0.2	100	15	1700
8	0.5	100	not reached	not reached

For a higher measurement rate, the overall delay until the MPP is reached increases. A lower rate for the measurement rate, in some situations the MPP is not reached or is reached within a tolerance.

The other setting that is influencing the MPPT algorithm performance and accuracy is the voltage step. By decreasing the voltage step, if it becomes too small, the delay until MPP is increasing dramatically. By increasing the voltage step, it can be observed that the delay until MPP is decreasing, but in some situations the maximum power point is never reached. The algorithm is oscillating around the MPP, but it cannot detect it precisely.

The application that is drawing the characteristic of the SAS is presented and it is referenced in section IV. The output characteristic is plotted on a graphic or the user can chose to export the data in CSV (comma-separated values) format file for further analysis.

The application can also be used for regular checking if the algorithm is correctly finding the right MPP. The accuracy of the algorithm depends on the chosen step value. The experiments revealed that the error is less than the step value by 10-45% when the MPP is reached.

VII. MPPT SIMULATION AND COMPARISON USING A SPECIFIC HARDWARE MPPT COMMERCIAL IC

LT8611 is a Synchronous Step-Down Integrated Converter [30] with a built-in MPPT algorithm. The setup introduced in Fig. 19 is using a simplified PV module model for the input power source (16 low current PV cells are connected in series).

The results are presented in Fig. 20. The incident irradiance steps from 200W/m^2 to 1000W/m^2 and the output voltage settles in about 1ms. This result is much faster than the average delay of 50 - 100ms from our MPP software controlled algorithm.

Arguably, our biggest challenge was the I/O latency's of the PC, as the electronic load instruction execution time is about 100µs. This explains that the main bottleneck of the implemented MPPT algorithm is the I/O transaction latency, the implementation should have a reduced number of I/O transactions. This was another strong argument for the IC MPPT algorithm we have chosen in our experiments.

VIII. CONCLUSION

In order to successfully test the MPPT algorithm, a hardware-in-the-loop test stand has been built based on a basic SAS. The electrical characteristics of the SAS were simulated and eventually tested using the custom developed software based on the reversed diode model simulations. The main benefit of using the SAS instead of radiation generator with real solar cells is given by the repeatability and the robustness at lower costs.

In the current form, the proposed system can be used for fast evaluation of different MPPT algorithms in the early stages of the design process. Also the system can be used for DC-DC convertor evaluation even with better results due to the shorter response time.

The main challenge for the incremental conductance algorithm implementation was the response time of the system (PC + bus + eLoad).

Running the initial calibration at different moments improved the performance of the IC algorithm, only minor delays being added to the execution time.

Furthermore, adding a tracking pre-regulator offers the possibility for the SAS to work in a much higher power range. The unique and novel way of implementing and testing the maximum tracking point algorithm offers a cost effective solution for prototyping in early phase of design of a complete PV system.

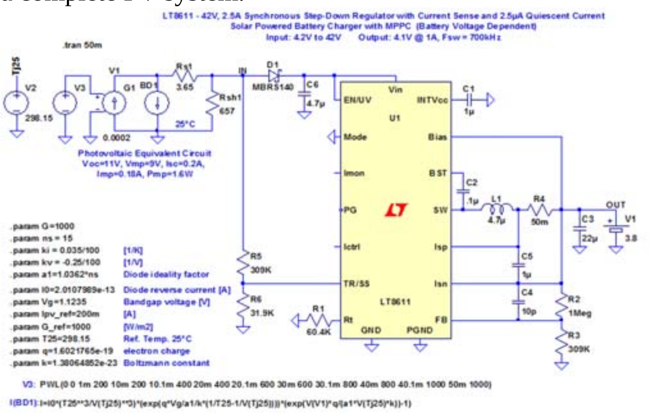

Figure 19. Hardware MPPT algorithm simulation schematic using LT8611

As future work, the authors intend to develop a DC-DC convertor using the MPPT algorithm presented here and will test it using the described setup. The use of gradient descent method was already taken into consideration for even faster and precise tracking process. An additional goal for the convertor is to provide dual input for a hybrid electrical power generation system based on PV modules and thermoelectric generators (TEGs).

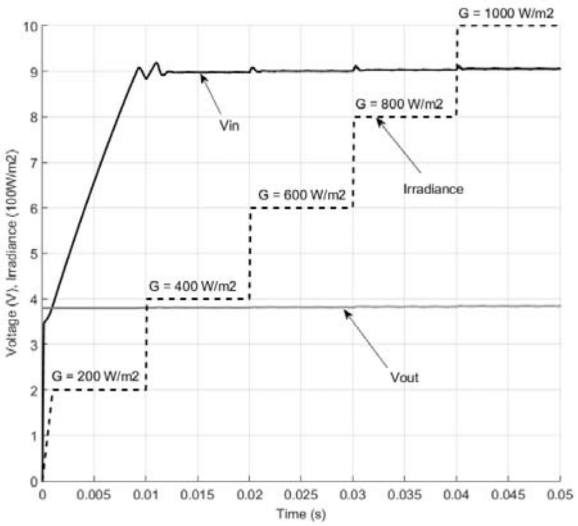

Figure 20. Hardware MPPT algorithm simulation results using LT8611

ACKNOWLEDGMENT

This work was supported by a grant of the Romanian National Authority for Scientific Research and Innovation, CNCS/CCCDI – UEFISCDI, project number PN-III-P2-2.1-PED-2016-0074, within PNCDI III.

REFERENCES

[1] S. Ghose, A. Uddin, K. Nandy, G. Uddin, "Photovoltaic Maximum Power Point Tracking Control System by using Microcontroller", Journal of Modern Science and Technology, Vol. 3 No.1 March 2015, 201-2013, pp. 201-213, ISSN: 2201-6686.

[2] E. Saloux, A. Teyssedou, M. Sortin, "Explicit model of photovoltaic panels to determine voltages and currents at the maximum power point", Solar Energy 85, 2011, pp. 713-722, DOI: 10.1016/j.solener.2010.12.022.

[3] D. P. Hohm, M. E. Ropp, "Comparative Study of Maximum Power Point Tracking Algorithms", Prog. Photovoltaic: Res. Appl. 2003, DOI: 10.1002/pip.459.

[4] J. L. Gray, "The Physics of the Solar Cell", in A. Luque, S. Hegedus, (Ed) "Hand book of photovoltaic science and Engineering", 2003 John Wiley & Sons Ltd., ISBN: 0-471-49196-9, pp. 61 - 112.

[5] B. K. Dey, I. Khan, N. Mandal, "Mathematical Moddeling and Characteristic analysis of solar PV Cell", Information Technology, Electronics and Mobile Communication Conference (IECOM), 2016, DOI: 10.1109/IEMCON.2016.7746318.

[6] S. A. Rahaman, R. K. Varma and T. Vanderheide, "Generalised Model Of Photovoltaic Panel", IET Renewable Power Generation, 2014, vol.8, Issue. 3, pp.217-229, DOI: 10.1049/iet-rpg.2013.0094

[7] N. Femia, G. Petrone, G. Spagnuolo, M. Vitelli, "Optimizing sampling rate of P&O MPPT technique", in Proc. IEEE PESC, 2004, pp.1945-1949, DOI: 10.1109/ICAIET.2014.48.

[8] T. Esram, Patrick L. Chapman, "Comparison of Photovoltaic Array Maximum Power Point Tracking Techniques", IEEE Transactions on Energy Conversion,Volume: 22, Issue: 2, June 2007, pp.439-449, DOI: 10.1109/TEC.2006.874230.

[9] T. R. Wellawatta, Y.-T. Seo, H.-H. Lee, Sung-Jin Choi, "A regulated incremental conductance MPPT algorithm for photovoltaic system", IEEE Energy Conversion Congress and Exposition (ECCE), Cincinnati, 2017, DOI: 10.1109/ECCE.2017.8096448.

[10] S. U. Ramani, S. K. Kollimalla, B. A., "Comparative study of P&O and incremental conductance method for PV system", International Conference on Circuit, Power and Computing Technologies (ICCPCT), Kollam, India, 2017, DOI: 10.1109/ICCPCT.2017.8074198.

[11] S. Gautam, D. B. Raut, P. Neupane, D. P. Ghale, R. Dhakal, "Maximum power point tracker with solar prioritizer in photovoltaic application", IEEE International Conference on Renewable Energy Research and Applications (ICRERA), Birmingham, 2017, DOI: 10.1109/ICRERA.2016.7884494.

[12] M. Unlu, S. Camur, E. Beser, B. Arifoglu, "A new method for tracking the global maximum power point for grid-connected PV system under partially shaded conditions", IEEE International Conference on Renewable Energy Research and Applications(ICRERA), Birmingham, 2016, pp. 867-872, DOI: 10.1109/ICRERA.2016.7884459.

[13] I. V. Banu, R. Beniuga, M. Istrate, "Comparative analysis of the perturb-and-observe and incremental conductance MPPT methods", 8TH International Symposium on advanced topics in electrical engineering (ATEE), Bucharest, 2013, pp. 1-4, DOI: 10.1109/ATEE.2013.6563483.

[14] G. Walker, "Evaluating MPPT converter topologies using a MATLAB PV model", J. Electr. Electron. Eng. Aust. 2001, 21(1), pp. 49 – 55.

[15] H.S. Rauschenbach, Solar Cell Array Design Handbook, The Principles and Technology of Photovoltaic Energy Conversion, Springer: New York, 1980; pp. 167-183, ISBN: 978-9401179171.

[16] K. Emery, Measurement and Characterization of Solar Cells and Modules, In Handbook of Photovoltaic Science and Engineering, 2nd ed.; Luque, A., Hegedus S., Eds.; John Wiley & Sons, United Kingdom, 2011, pp. 1164, ISBN 978-0-470-72169-8, pp. 797–840.

[17] J.A. Gow, C.D. Manning, "Development of a photovoltaic array model for use in power-electronics simulation studies", IEE Proc. – El. Power App. 1999, 146(2), pp. 193 – 200, DOI: 10.1049/ip-epa: 19990116.

[18] M.P. Aparicio, J.T. Pelegrí-Sebastiá Sogorb, V. Llario, Modeling of Photovoltaic Cell Using Free Software Application for Training and Design Circuit in Photovoltaic Solar Energy, In New Developments in Renewable Energy, Arman H., Yuksel I., Eds., Intech: Vienna, Austria, 2013, pp. 121 – 139, ISBN 978-953-51-1040-8.

[19] S. Sumathi, L.A. Kumar, P. Surekha, Solar PV and Wind Energy Conversion Systems. An Introduction to Theory, Modeling with MATLAB/SIMULINK, and the Role of Soft Computing Techniques, Springer: Switzerland, 2015, pp. 59-144, ISBN-13: 978-3319149400.

[20] T. Khatib, W. Elmenreich, Modeling of Photovoltaic Systems Using MATLAB: Simplified Green Codes, John Wiley & Sons: Hoboken, New Jersey, US, 2016, pp. 39 - 88, ISBN-13: 978-1119118107.

[21] M.G. Villalva, J.R. Gazoli, E.R. Filho, "Comprehensive Approach to Modeling and Simulation of Photovoltaic Arrays", IEEE T. Power Electr. 2009, 24(5), pp. 1198 – 1208, DOI: 10.1109/TPEL.2009. 2013862.

[22] W. Kim, W. Choi, "A novel parameter extraction method for the one-diode solar cell model", Sol Energy 2010, 84(6), pp. 1008 – 1019, DOI: 10.1016/j.solener.2010.03.012.

[23] J. Cubas, S. Pindado, C. de Manuel, "Explicit Expressions for Solar Panel Equivalent Circuit Parameters Based on Analytical Formulation and the Lambert W-Function", Energies 2014, 7, pp. 4098 – 4115, DOI: 10.3390/ece-1-c013.

[24] A. Gontean, S. Lica, S. Bularka, R. Szabo, D. Lascu, "A Novel High Accuracy PV Cell Model Including Selfheating and Parameter Variation", Energies 2018, DOI: 10.3390/en11010036.

[25] J. Clarke, "12 V 20-120W Solar Panel Simulator", Silicon Chip Magazine, March 2011, pp. 74-81.

[26] K.H. Hussein, I. Muta, T. Hoshino, M. Osakada, "Maximum photovoltaic power tracking: an algorithm for rapidly changing atmospheric conditions, IEE Proceedings - Generation, Transmission and Distribution", Vol: 142, Issue: 1, Jan 1995, pp: 59 – 64, DOI: 10.1049/ip-gtd:19951577.

[27] M. Rosu-Hamzescu, S. Oprea, "Practical Guide to implementing Solar Panel MPPT algorithms", Microchip, AN1521.

[28] Yuan. X, Zhao Y, Zhu W. "Real-Time Simulation and Research on Photovoltaic Power System based on RT-LAB", The Open Fuels & Energy Science Journal, 2015, 8:183-188, DOI: 10.2174/1876973X01508010183

[29] Rajesh P, Rajasekar S, Rajesh G, Paulson S, Solar Array System Simulation using FPGA with Hardware Co-Simulation", International Symposium on Industrial Electronics , DOI: 10.1109/ISIE.2014.6864975

[30] Linear Technology, LT8611 datasheet, http://cds.linear.com/docs/en/datasheet/8611fa.pdf, (last visited 2 Dec 2017)

[31] Photovoltaic cell IHUAX.CN, 5.2W A++ 156mm monocrystalline solar cell, https://www.aliexpress.com/item/50pcslot-4-6W-156mm-mono-solar-cells-6x6-150feet-Tabbing-Wire-15feet-Busbar-Wire-1pc/1932804007.html, Last visited 21 Sep 2017

[32] H&H Electronic Load datasheet, PLA Series, http://www.hoecherl-hackl.com/datenblatt/14/PLA212.html, (Last visited 2 Dec 2017)